

See discussions, stats, and author profiles for this publication at: <https://www.researchgate.net/publication/5540348>

Chemical compounds formed from diacetylene and rare-gas atoms: HKrC₄H and HXeC₄H

ARTICLE *in* JOURNAL OF THE AMERICAN CHEMICAL SOCIETY · JANUARY 2004

Impact Factor: 12.11 · DOI: 10.1021/ja038610x · Source: PubMed

CITATIONS

71

READS

20

5 AUTHORS, INCLUDING:



Jan Lundell

University of Jyväskylä

119 PUBLICATIONS 3,728 CITATIONS

SEE PROFILE



Harri Kiljunen

University of Helsinki

7 PUBLICATIONS 376 CITATIONS

SEE PROFILE



Markku Rasanen

University of Helsinki

267 PUBLICATIONS 6,961 CITATIONS

SEE PROFILE

Chemical Compounds Formed from Diacetylene and Rare-Gas Atoms: HKrC₄H and HXeC₄H

Hanna Tanskanen,^{*,†} Leonid Khriachtchev,[†] Jan Lundell,[†] Harri Kiljunen,[‡] and Markku Räsänen[†]

Contribution from the Department of Chemistry, University of Helsinki, P.O. Box 55, FIN-00014, Finland, and VERIFIN, University of Helsinki, P.O. Box 55, FIN-00014, Finland

Received September 19, 2003; E-mail: hanna.tanskanen@helsinki.fi

Abstract: New organic rare-gas compounds, HRgC₄H (Rg = Kr or Xe), are identified in matrix-isolation experiments supported by ab initio calculations. These compounds are the largest molecules among the known rare-gas hydrides. They are prepared in low-temperature rare-gas matrixes via UV photolysis of diacetylene and subsequent thermal mobilization of H atoms at ~30 and 45 K for Kr and Xe, respectively. The strongest IR absorption bands of the HRgC₄H molecules are the H–Rg stretches with the most intense components at 1290 cm⁻¹ for HKrC₄H and at 1532 cm⁻¹ for HXeC₄H, and a number of weaker absorptions (C–H stretching, C–C–C bending, and C–C–H bending modes) are also found in agreement with the theoretical predictions. As probably the most important result, the IR absorption spectra indicate some further stabilization of the HRgC₄H molecules as compared with the corresponding HRgC₂H species identified recently (Khriachtchev et al. *J. Am. Chem. Soc.* **2003**, *125*, 4696 and Khriachtchev et al. *J. Am. Chem. Soc.* **2003**, *125*, 6876). The computational energetic results support this trend. HXeC₄H is predicted to be 2.5 eV lower in energy than H + Xe + C₄H, which is ~1 eV larger than the corresponding value for HXeC₂H. We expect that the larger molecules HRgC₆H and HRgC₈H are even more stable and the HRgC_{2n}H species are good candidates for bulk organic rare-gas material.

1. Introduction

The first xenon-containing compound was reported by Bartlett in 1962.¹ After this pioneering work, a large number of Xe and Kr derivatives were synthesized,^{2–5} and among them XeF₂ and KrF₂ are probably the best known.^{6,7} One of the important developments in rare-gas chemistry was the finding of rare-gas hydrides HRgY, where Rg is a rare-gas atom and Y is an electronegative fragment. These chemically bound HRgY molecules have been prepared in low-temperature rare-gas matrixes by photolyzing HY precursors and then mobilizing H atoms thermally.^{8,9} Use of this procedure has led to the preparation of compounds such as HArF,^{10,11} HKrF,¹² HXeO,¹³

HXeCN, and HKrCN¹⁴. In addition to the monomeric HRgY molecules, some of their complexes (with H₂O and N₂) have recently been isolated in rare-gas matrixes.^{15–17}

In organic chemistry rare-gas compounds, especially XeF₂⁶ and XeF₄¹⁸ have been used in the synthesis of compounds with a Xe–C bond.^{3,4} Organoxenonium salts have been considered to offer promising access to Xe–C compounds due to their lower oxidation potential in comparison with the [FXe]⁺ cation.³ At the present time, various types of organoxenon compounds are known: mononuclear xenonium(II) salts [RXe]⁺[Y][–] (where R = aryl, polyfluoroalkenyl, alkynyl and Y = a counteranion), binuclear xenonium(II) salts [(C₆F₅Xe)₂Z]⁺[AsF₆][–] (where Z = F or Cl), arylxenonium(IV) salt [C₆F₅XeF₂]⁺[BF₄][–], covalent xenon(II) compounds C₆F₅XeZ [where Z = F, Cl, CN, or OC(O)C₆F₅], symmetric and asymmetrical diorganoxenon(II) compounds, R₂Xe (where R = C₆F₅ or 2,4,6-C₆H₂F₃), and RXeR' (where R = C₆F₅ and R' = 2,4,6-C₆H₂F₃), respectively.³ Recently, Frohn and Bardin have reported the preparation of the alkynylxenon(II) compound, [CF₃C≡CXe][BF₄].¹⁹

First predictions for fluorine-free alkynylxenon derivatives were presented by Lundell et al.²⁰ They reported theoretically

[†] Department of Chemistry.

[‡] VERIFIN.

- (1) Bartlett, N. *Proc. Chem. Soc.* **1962**, 218.
- (2) Holloway, J. H.; Hope, E. G. *Adv. Inorg. Chem.* **1999**, *46*, 51.
- (3) Frohn, H.-J.; Bardin, V. V. *Organometallics* **2001**, *20*, 4750.
- (4) Brel, V. K.; Pirkuliev, N. Sh.; Zefirov, N. S. *Russ. Chem. Rev.* **2001**, *70*, 231.
- (5) Lehmann, J. F.; Mercier, H. P.; Schrobilgen, G. J. *Coord. Chem. Rev.* **2002**, *233–234*, 1.
- (6) Hoppe, R.; Dähne, W.; Mattauch, M.; Rödder, K. H. *Angew. Chem.* **1962**, *74*, 903.
- (7) Turner, J. J.; Pimentel, G. C. *Science* **1963**, *140*, 974.
- (8) Pettersson, M.; Lundell, J.; Räsänen, M. *Eur. J. Inorg. Chem.* **1999**, 729.
- (9) Lundell, J.; Khriachtchev, L.; Pettersson, M.; Räsänen, M. *Low Temp. Phys.* **2000**, *26*, 680.
- (10) Khriachtchev, L.; Pettersson, M.; Runeberg, N.; Lundell, J.; Räsänen, M. *Nature (London)* **2000**, *406*, 874.
- (11) Khriachtchev, L.; Pettersson, M.; Lignell, A.; Räsänen, M. *J. Am. Chem. Soc.* **2001**, *123*, 8610.
- (12) Pettersson, M.; Khriachtchev, L.; Lignell, A.; Räsänen, M.; Bihary, Z.; Gerber, R. B. *J. Chem. Phys.* **2002**, *116*, 2508.
- (13) Khriachtchev, L.; Pettersson, M.; Lundell, J.; Tanskanen, H.; Kiviniemi, T.; Runeberg, N.; Räsänen, M. *J. Am. Chem. Soc.* **2003**, *125*, 1454.

- (14) Pettersson, M.; Lundell, J.; Khriachtchev, L.; Räsänen, M. *J. Chem. Phys.* **1998**, *109*, 618.
- (15) Nemukhin, A. V.; Grigorenko, B. L.; Khriachtchev, L.; Tanskanen, H.; Pettersson, M.; Räsänen, M. *J. Am. Chem. Soc.* **2002**, *124*, 10706.
- (16) Lignell, A.; Khriachtchev, L.; Pettersson, M.; Räsänen, M. *J. Chem. Phys.* **2002**, *117*, 961.
- (17) Lignell, A.; Khriachtchev, L.; Pettersson, M.; Räsänen, M. *J. Chem. Phys.* **2003**, *118*, 11120.
- (18) Claassen, H. H.; Selig, H.; Malm, J. G. *J. Am. Chem. Soc.* **1962**, *84*, 3593.
- (19) Frohn, H.-J.; Bardin, V. V. *Chem. Commun.* **2003**, 2352.

the stability and spectroscopic properties of HXeC_2H , HXeCCXeH , and some other organoxenon compounds.²⁰ Recently, in experiments with acetylene in solid Xe, we have prepared and identified the new organoxenon compounds HXeCC , HXeC_2H , and HXeCCXeH .²¹ The HXeC_2H molecule was also simultaneously reported by Feldman et al.²² Importantly, these compounds do not contain fluorine, which distinguishes them from previously experimentally prepared organoxenon species.³ In comparison with xenon, organic compounds containing krypton are very exceptional,⁵ and so far only one neutral Kr-containing organic molecule is known to our best knowledge,^{2,5,23} and this is the recently reported HKrC_2H molecule.²³ The other two known species with a Kr–C bond are the CH_3Kr^+ cation²⁴ and the inorganic HKrCN molecule.¹⁴

An important challenge for future research is the preparation of larger organic molecules containing rare-gas atoms. Indeed, the most important activity and applications of organic chemistry involve structures with large numbers of atoms. In our recent work,²³ we predicted particularly the stability of HKrC_4H and HKrC_3H_3 molecules, and their Xe analogues are most probably stable as well. Because the electron affinity of the Y fragment plays an important role in the formation and the stabilization of the HRgY molecules,⁸ even larger organic rare-gas species of this type are possible to prepare. In fact, the electron affinity of the C_{2n}H radicals increases with n .²⁵ This intuitively suggests that the HRgC_{2n}H molecules should become more stable with increasing n . More generally, one can expect that various structures of $\text{HRgC}\equiv\text{R}$ exist, if a large (≥ 3 eV) electron affinity is localized at the carbon atom of the $\text{C}\equiv\text{R}$ radical.

In this work, we investigate this question and report the preparation of two novel organic rare-gas compounds, HKrC_4H and HXeC_4H . These molecules and their deuterated isotopologues are identified by using IR absorption spectroscopy and ab initio calculations. HKrC_4H and HXeC_4H are new members in the expanding group of alkynyl-rare-gas derivatives.

2. Computations

Computational Details. All calculations were performed with the Gaussian 98 (revision A.11.4) package of computational codes.²⁶ Electron correlation was considered via the Møller–Plesset second-order perturbation theory (MP2). Relativistic pseudopotentials (ECP) by LaJohn et al. were used to describe xenon.²⁷ This ECP includes the d-subshell in valence space resulting in 18 valence electrons, and it was used in a decontracted form. This basis set is denoted as LJ18.

- (20) Lundell, J.; Cohen, A.; Gerber, R. B. *J. Phys. Chem. A* **2002**, *106*, 11950.
- (21) Khriachtchev, L.; Tanskanen, H.; Lundell, J.; Pettersson, M.; Kiljunen, H.; Räsänen, M. *J. Am. Chem. Soc.* **2003**, *125*, 4696.
- (22) Feldman, V. I.; Sukhov, F. F.; Orlov, A. Y.; Tyulpina, I. V. *J. Am. Chem. Soc.* **2003**, *125*, 4698.
- (23) Khriachtchev, L.; Tanskanen, H.; Cohen, A.; Gerber, R. B.; Lundell, J.; Pettersson, M.; Kiljunen, H.; Räsänen, M. *J. Am. Chem. Soc.* **2003**, *125*, 6876.
- (24) Hovey, J. K.; McMahon T. B. *J. Phys. Chem.* **1987**, *91*, 4560.
- (25) Taylor, T. R.; Xu, C. S.; Neumark, D. M. *J. Chem. Phys.* **1998**, *108*, 10018.
- (26) Frisch, M. J.; Trucks, G. W.; Schlegel, H. B.; Scuseria, G. E.; Robb, M. A.; Cheeseman, J. R.; Zakrzewski, V. G.; Montgomery, J. A., Jr.; Stratmann, R. E.; Burant, J. C.; Dapprich, S.; Millam, J. M.; Daniels, A. D.; Kudin, K. N.; Strain, M. C.; Farkas, O.; Tomasi, J.; Barone, V.; Cossi, M.; Cammi, R.; Mennucci, B.; Pomelli, C.; Adamo, C.; Clifford, S.; Ochterski, J.; Petersson, G. A.; Ayala, P. Y.; Cui, Q.; Morokuma, K.; Malick, D. K.; Rabuck, A. D.; Raghavachari, K.; Foresman, J. B.; Cioslowski, J.; Ortiz, J. V.; Stefanov, B. B.; Liu, G.; Liashenko, A.; Piskorz, P.; Komaromi, I.; Gomperts, R.; Martin, R. L.; Fox, D. J.; Keith, T.; Al-Laham, M. A.; Peng, C. Y.; Nanayakkara, A.; Gonzalez, C.; Challacombe, M.; Gill, P. M. W.; Johnson, B. G.; Chen, W.; Wong, M. W.; Andres, J. L.; Head-Gordon, M.; Replogle, E. S.; Pople, J. A. *Gaussian 98*, revision A.11.4; Gaussian, Inc.: Pittsburgh, PA, 1998.
- (27) LaJohn, L. A.; Christiansen, P. A.; Ross, R. B.; Atashroo, T.; Ermler, W. C. *J. Chem. Phys.* **1987**, *87*, 2812.

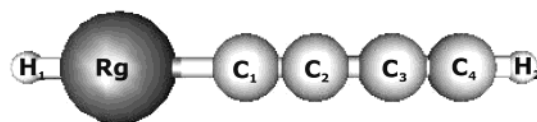


Figure 1. Structure of the HRgC_4H molecules ($\text{Rg} = \text{Kr}$ or Xe). The computed parameters are given in Table 1.

Table 1. Equilibrium Structures, NBO Charges, and Dipole Moments of HKrC_4H and HXeC_4H ^a

	HKrC_4H	HXeC_4H
$r(\text{H}_1\text{--Rg})$	1.5810	1.7406
$r(\text{Rg--C}_1)$	2.2551	2.3293
$r(\text{RgC}_1\text{--C}_2)$	1.2360	1.2350
$r(\text{C}_2\text{--C}_3\text{C}_4\text{H}_2)$	1.3692	1.3678
$r(\text{C}_3\text{--C}_4\text{H}_2)$	1.2211	1.2212
$r(\text{C}_4\text{--H}_2)$	1.0596	1.0598
$q(\text{H}_1)$	0.005	−0.152
$q(\text{Rg})$	0.560	0.767
$q(\text{C}_1)$	−0.320	−0.427
$q(\text{C}_2)$	−0.185	−0.153
$q(\text{C}_3)$	−0.099	−0.056
$q(\text{C}_4)$	−0.178	−0.198
$q(\text{H}_2)$	0.218	0.219
$\mu(\text{Debye})$	4.23	3.60

^a The bond lengths are in Å. The notation of the atoms is shown in Figure 1.

The standard 6-311++G(2d,2p) basis set was used for hydrogen, carbon, and krypton. The harmonic vibrational frequencies were calculated analytically using the standard electronic structure algorithms. This computational level has been repeatedly used to simulate HRgY molecules, and it has exhibited good agreement with experiment.^{8,9,21,23}

Computational Results: HKrC_4H . The calculations show that HKrC_4H is a true energy minimum on the potential surface. The linear equilibrium structure of HKrC_4H is presented in Figure 1, and the structural parameters are collected in Table 1. The H–Kr and Kr–C distances are 1.58 and 2.26 Å, respectively, which are similar to the corresponding values of HKrC_2H (1.60 and 2.25 Å calculated at the same level of theory). The partial charges of the HKrC_4H molecule were calculated using natural bond orbital (NBO) analysis at the MP2/6-311++G(2d,2p) level, and the results are also presented in Table 1. The NBO analysis indicates strong ionic character for HKrC_4H , with a positive charge of +0.56 on Kr and negative charges of −0.32 and −0.19 on C_1 and C_2 atoms. Comparing the charge values of HKrC_4H with values of HKrC_2H (+0.55 on Kr and −0.40, −0.33 on the C atoms), we could see that in the case of HKrC_4H the positive charge on Kr slightly increases and the negative partial charges are distributed among the four C atoms.

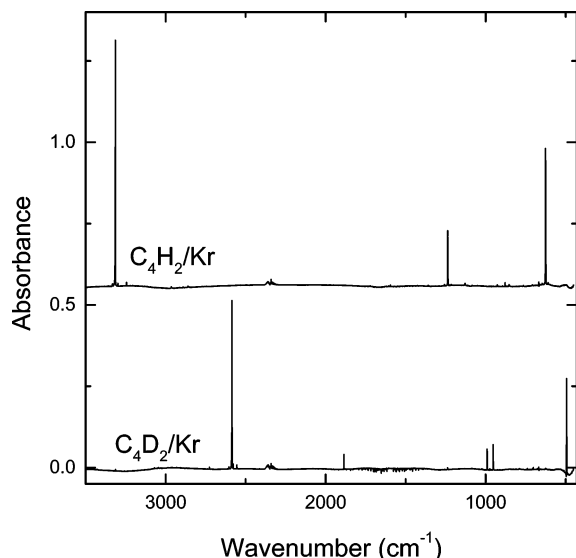
The computed harmonic frequencies and IR intensities of the HKrC_4H and DKrC_4D molecules are given in Table 2. The H–Kr and Kr–C stretching frequencies at the MP2/6-311++G(2d,2p) level for HKrC_4H are 1517 and 238 cm^{-1} , respectively, and for DKrC_4D the corresponding values are 1080 and 236 cm^{-1} , respectively. The H(D)–Kr stretching absorptions are very strong, which is generally characteristic for HRgY molecules.^{8,9} The HKrC_4H molecule is by 1.3 eV lower in energy than the separate fragments $\text{H} + \text{Kr} + \text{C}_4\text{H}$, which allows its annealing-induced formation from these fragments. Similarly to other HRgY molecules, HKrC_4H is a metastable high-energy species, being 5.7 eV above the energy limit of the $\text{C}_4\text{H}_2 + \text{Kr}$ constituents.

Computational Results: HXeC_4H . The equilibrium structural parameters and NBO-computed partial charges of this molecule are presented in Table 1. At the MP2 level, the H–Xe bond distance is 1.74 Å, and the Xe–C bond is 2.33 Å long, and these values are similar to those of HXeC_2H (1.75 and 2.32 Å).²⁰ The calculated charge on Xe is +0.77, and the H atom bound to the Xe atom has a negative charge of −0.15. Most of the negative partial charge is located in the C_4H group.

Table 2. Calculated MP2/6-311++G(2d,2p) Vibrational Frequencies (in cm^{-1}) and IR Intensities in Parentheses (in km mol^{-1}) of HKrC_4H and HXeC_4H^a

	HKrC_4H	DKrC_4D	HXeC_4H	DXeC_4D
C–H(D) stretch	3484.7 (100.0)	2670.4 (84.8)	3482.3 (98.7)	2668.9 (83.1)
C–C stretch	2140.5 (6.8)	2104.8 (0.4)	2161.2 (3.4)	2136.0 (0.4)
	1979.9 (23.6)	1909.8 (14.9)	2007.3 (25.8)	1927.2 (19.5)
H(D)–Kr(Xe) stretch	1517.2 (3173.9)	1080.2 (1498.0)	1759.2 (1898.4)	1248.9 (930.9)
C–C–C bend	931.2 (132.6)	914.5 (224.5)	949.4 (113.1)	933.8 (134.0)
C–C–H(D) bend	590.3 (49.2) ^b	455.8 (26.6) ^b	664.0 (10.6) ^b	496.7 (17.5) ^b
			591.2 (49.2) ^b	458.6 (18.2) ^b
C–Kr(Xe) stretch	238.0 (161.3)	236.1 (157.5)	235.0 (118.7)	232.8 (115.9)

^a Only the most intense absorptions are presented. ^b Doubly degenerate.

**Figure 2.** IR absorption spectra of diacetylene ($\sim 1:1000$) in solid Kr at 8 K. Spectra for C_4H_2 and C_4D_2 are shown by the upper and lower traces, respectively.

The calculated harmonic frequencies of HXeC_4H and DXeC_4D at the MP2 level are presented in Table 2. The H–Xe stretching frequency of HXeC_4H is 1759 cm^{-1} , and the Xe–C stretching frequency is 235 cm^{-1} . For DXeC_4D , the predicted frequencies are 1249 and 233 cm^{-1} , respectively. The computed H–Xe stretching frequency is quite typical for known xenon-containing hydrides.^{8,9} For example, the corresponding value is 1740 cm^{-1} for HXeCl , 1683 cm^{-1} for HXeOH , and 1679 cm^{-1} for HXeBr .⁹ The HXeC_4H molecule is computationally lower by $\sim 2.5\text{ eV}$ in energy than $\text{H} + \text{Xe} + \text{C}_4\text{H}$, which allows its annealing-induced formation from these fragments in the experiment. Similarly to other HRgY compounds, HXeC_4H is a metastable species with an energy of 4.5 eV above the energy limit of separated diacetylene and xenon.

3. Experimental Section

Experimental Details. The $\text{C}_4\text{H}_2/\text{Kr}$ and $\text{C}_4\text{H}_2/\text{Xe}$ samples were deposited from the gas phase onto a CsI window cooled by a closed-cycle helium cryostat (DE-202A, APD) at 20 and 30 K, respectively. After deposition, the samples were cooled to 8 K and photolyzed. The sample ratios of $\text{C}_4\text{H}_2/\text{Kr}$ and $\text{C}_4\text{H}_2/\text{Xe}$ were typically $\sim 1:1000$ to $1:2000$, which produced monomeric diacetylene in matrixes. The matrix thickness was typically $\sim 100\text{ }\mu\text{m}$. Diacetylene (C_4H_2) was synthesized using the method described by Armitage et al.,²⁸ and diacetylene- d_2 was prepared with the method used by Bondybey and English.²⁹ The diacetylene- d_2 sample contained practically no diacetylene- d as shown by the recorded IR absorption spectrum (Figure 2).

The IR absorption spectra in the $4000\text{--}400\text{ cm}^{-1}$ region were measured with a Nicolet 60 SX FTIR spectrometer with a resolution

of 1 cm^{-1} co-adding 500 or 1000 scans. The photolysis was carried out using an excimer laser (MPB, MSX-250) operating at 193 nm (ArF) and an optical parametric oscillator (Continuum, OPO Sunlite) at 250, 240, and 235 nm.

Experimental Results: $\text{C}_4\text{H}_2/\text{Kr}$ Matrix. The IR absorption spectra of C_4H_2 (the strongest absorptions at 3314, 1237.5, and 626 cm^{-1}) and C_4D_2 (2585.5, 1886, 990.5, 953, and 494.5 cm^{-1}) in a Kr matrix are presented in Figure 2 (see the upper and lower traces, respectively), showing mainly monomeric trapping. These values agree, taking into account normal matrix shifts, with the spectrum of diacetylene obtained by Patten and Andrews in solid Ar.³⁰ Diacetylene in solid Kr was photolyzed by 235, 240, and 250 nm radiation. Typically, photolysis at 235 nm (7.4×10^3 pulses, $\sim 2\text{ mJ/cm}^2$) decomposed about 50% of C_4H_2 . It should be remembered that UV photolysis in rare-gas solids is often self-limited due to rising absorbers,³¹ and this was found in the present case as well. The products forming upon UV photolysis of diacetylene are C_4H radicals (2055 cm^{-1}),³² carbon clusters such as C_4 (1539.5 cm^{-1})³³ and C_8 (2065.5 cm^{-1}),³³ and also some other hydrocarbons. C_4H appears in the initial stage of photolysis, reaches its maximum, and then decreases. The C_4 concentration increases monotonically. Importantly, we did not detect KrHKr^+ ions (absorbing at 852 and 1008 cm^{-1})^{34,35} after photolysis at 240 and 250 nm, whereas this species is seen after photolysis at 235 nm.

Formation of Kr-containing molecules with charge-transfer character is known to require a strongly electronegative species to be present in the matrix after photolysis.^{8,9} The fragment with the large electron affinity in this study is C_4H (EA $\approx 3.6\text{ eV}$).²⁵ Upon annealing of the photolyzed sample at $\sim 30\text{ K}$, the H atoms become mobile,³⁶ and they can react with the Kr + C_4H centers. Accordingly, annealing of the photolyzed $\text{C}_4\text{H}_2/\text{Kr}$ matrix yields prominent absorption bands at 1275, 1290 (the strongest band), 1307, and 1317 cm^{-1} . These absorptions are assigned to the H–Kr stretching mode of the HKrC_4H molecule. Upon deuteration, the corresponding absorption bands are at 961.5 (the strongest band) and 977 cm^{-1} . Typical IR absorption spectra after photolysis and thermal mobilization of H atoms are presented in Figure 3. A number of weaker absorptions correlating with the strongest bands were also found in the spectra (see Table 3). The weaker bands of the same absorber are identified using its selective decomposition at 350 nm, as was successfully applied elsewhere.^{15,21,23,37} No corresponding absorption bands with normal matrix shifts are detected in analogous experiments with a $\text{C}_4\text{H}_2/\text{Ar}$ matrix (without doping with Kr). Preparation of the HKrC_4H molecule in solid Ar is complicated by inefficient complexation of C_4H_2 with Kr in an Ar matrix and by decomposition of C_4H radicals upon UV photolysis.

(30) Patten, K. O.; Andrews, L. *J. Phys. Chem.* **1986**, 90, 3910.

(31) Khriachtchev, L.; Pettersson, M.; Räsänen, M. *Chem. Phys. Lett.* **1998**, 288, 727.

(32) Dismuke, K. I.; Graham, W. R. M.; Weltner, W. *J. Mol. Spectrosc.* **1975**, 57, 127.

(33) Szczepanski, J.; Ekern, S.; Chapo, C.; Vala, M. *Chem. Phys.* **1996**, 211, 359.

(34) Bondybey, V. E.; Pimentel, G. C. *J. Chem. Phys.* **1972**, 56, 3832.

(35) Milligan, D. E.; Jacox, M. E. *J. Mol. Spectrosc.* **1973**, 46, 460.

(36) Eberlein, J.; Creuzburg, M. *J. Chem. Phys.* **1997**, 106, 2188.

(37) Khriachtchev, L.; Tanskanen, H.; Pettersson, M.; Räsänen, M.; Ahokas, J.; Kunttu, H.; Feldman, V. *J. Chem. Phys.* **2002**, 116, 5649.

(28) Armitage, J. B.; Jones, E. R. H.; Whiting, M. C. *J. Chem. Soc.* **1951**, 44.

(29) Bondybey, V. E.; English, J. H. *J. Chem. Phys.* **1979**, 71, 777.

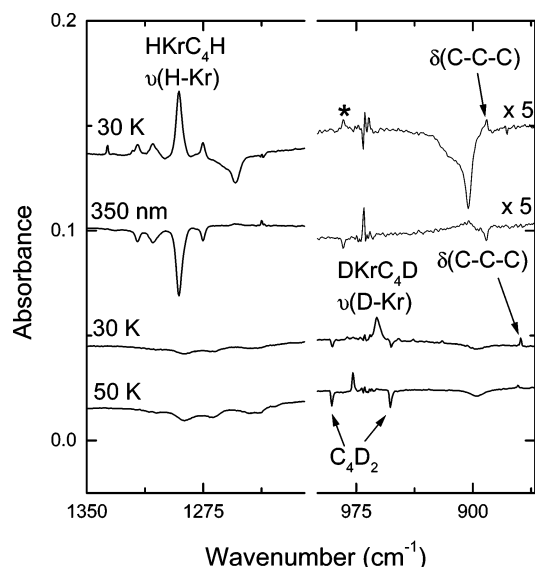


Figure 3. Difference IR absorption spectra of HKrC₄H in solid Kr. Shown are the result of annealing the photolyzed sample at 30 K (the upper trace), the result of 350 nm irradiation of the annealed sample (the second trace from top), and the results of annealing the photolyzed deuterated samples at 30 and 50 K (the two lower traces). The spectra are measured at 8 K. The absorption band marked with an asterisk (*) is not assigned here to the HKrC₄H molecule because this is not supported by the deuteration experiments and calculations. Additional spectral features originate from background fluctuations.

Table 3. Observed IR Absorptions of HKrC₄H and HXeC₄H and Their Deuterated Isotopologues (in cm⁻¹)^a

	HKrC ₄ H	DKrC ₄ D	HXeC ₄ H	DXeC ₄ D
C–H(D) stretch	<i>b</i>	2582	3313	2581
			3316 (s)	2582.5 (s)
H(D)–Kr(Xe) stretch	1275.5	961.5	1503.5	1093
	1290	977 (s)	1521.5	1103.5
	1307.5		1532	1111.5
	1317 (s)		1545 (s)	1120.5 (s)
			1558.5 (s)	1127.5 (s)
C–C–C bend	892	869	896	863.5
		871 (s)	897.5 (s)	869.5 (s)
C–C–H(D) bend	587	<i>c</i>	586	<i>c</i>
	592.5		587.5	
			588.5(s)	
			590.5(s)	

^a The (s) mark refers to the absorption bands observed after the higher-temperature annealing. ^b For HKrC₄H we could not detect the C–H stretching vibration because it was most probably overlapping with the strong C–H stretch of diacetylene. ^c The low sensitivity of our apparatus in the spectral range below 500 cm⁻¹ did not allow us to detect the C–C–D bending vibrations.

Further annealing of the photolyzed C₄H₂/Kr sample at higher temperatures of ~40–50 K changes the spectrum considerably as presented in Figure 3 for the deuterated species (see Table 3 for details). The absorptions at 1275, 1290, and 1307 cm⁻¹ of the HKrC₄H molecule (961.5 cm⁻¹ for DKrC₄D) decrease and the absorption at 1317 cm⁻¹ (977 cm⁻¹ for DKrC₄D) increases during the higher-temperature annealing. A thermal modification of the absorption profile is also observed for the C–C–C bending mode.

Experimental Results: C₄H₂/Xe Matrix. The spectra of C₄H₂ (3305, 1234.5, and 624 cm⁻¹) and C₄D₂ (2579.5, 1181.5, 988, 951, and 492 cm⁻¹) in solid Xe agree with our spectra in solid Kr (see Figure 2) and the data of Patten and Andrews obtained in solid Ar.³⁰ The diacetylene/Xe matrices were photolyzed at various wavelengths (193, 240, or 250 nm). The 250 nm photolysis was found to be the most efficient, and after 4000 pulses (~10 mJ/cm²) over 50% of C₄H₂ was decomposed for a typical matrix thickness of 100 μm. The known self-

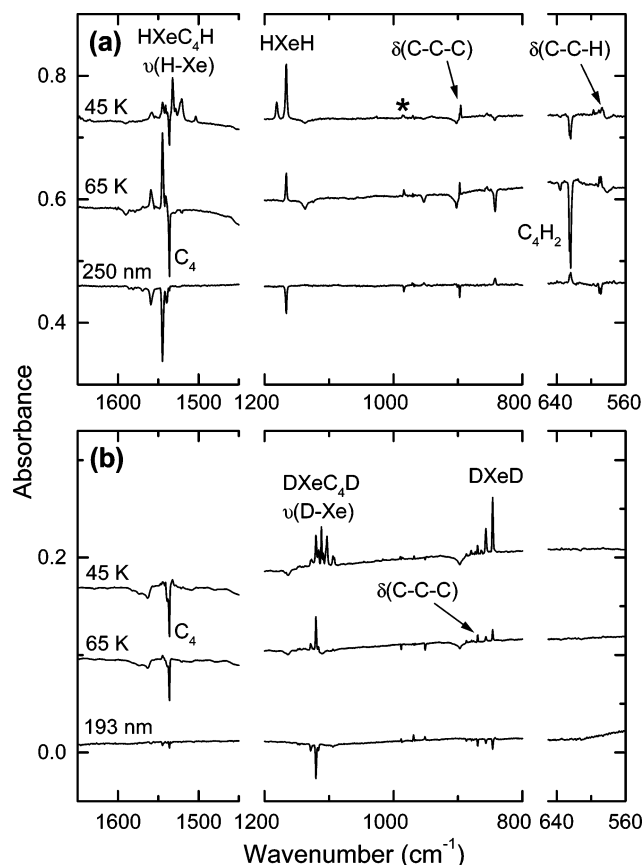


Figure 4. Difference IR absorption spectra of HXeC₄H (a) and DXeC₄D (b) in solid Xe. The spectra are measured at 8 K. (a) Shown are the result of annealing the photolyzed sample at 45 K (the upper trace), the result of annealing the already annealed (45 K) sample at 65 K (the middle trace), and the result of 250 nm irradiation of the annealed sample (the lower trace). The absorption band marked with an asterisk (*) is not assigned here to the HXeC₄H molecule because this is not supported by the deuteration experiments and calculations. (b) Shown are the results of annealing the photolyzed sample first at 45 K and then at 65 K (the two upper traces), and the result of short 193 nm irradiation of the annealed sample (the lower trace).

limitation process limits the photodissociation rate of diacetylene for longer photolysis and thicker and more concentrated samples.³¹ Upon photolysis of diacetylene in solid Xe, the IR absorption spectrum shows the appearance of C₄H radicals (2050 cm⁻¹)³² as well as carbon clusters such as C₄ (1536 cm⁻¹)³³ and C₈ (2057 cm⁻¹).³³ The formation kinetics of C₄H and C₄ is comparable with the case of Kr. XeHXe⁺ ions (953, 842.5, and 730.5 cm⁻¹)³⁸ are also produced in the photolysis.

Upon annealing of the photolyzed sample at 40–45 K, the atomic hydrogen becomes mobile,³⁶ leading to diffusion-controlled formation of HXeY molecules in a reaction with neutral Xe–Y centers;⁹ Y is C₄H in this case. Accordingly, we observed the annealing-induced formation of several unreported IR absorption bands (see Figure 4), in addition to the known absorptions of HXeH (1166 and 1180 cm⁻¹).³⁹ These new systematically appearing bands have the most intense components at 1503.5, 1521.5, 1532 (the strongest band), 1545, and 1558.5 cm⁻¹. Deuteration leads to bands at 1093, 1103.5, 1111.5 (the strongest band), 1120.5, and 1228 cm⁻¹. No corresponding bands with normal matrix shifts are found in analogous experiments in Ar and Kr matrixes, which suggests that these absorbers are due to novel Xe-containing species. We assign these absorptions to the H–Xe and D–Xe stretching modes of HXeC₄H and DXeC₄D, respectively. In addition,

(38) Kunttu, H.; Seetula, J.; Räsänen, M.; Apkarian, V. A. *J. Chem. Phys.* **1992**, 96, 5630.

(39) Pettersson, M.; Lundell, J.; Räsänen, M. *J. Chem. Phys.* **1995**, 103, 205.

weaker absorptions at 586, 587.5, 896, and 3313 cm^{-1} in the spectra (863.5 and 2581 cm^{-1} with deuteration) are observed to correlate with the stronger bands, and their assignments are presented in Table 3.

Similarly to the case of HKrC_4H , higher-temperature annealing (~ 55 – 70 K) changes the spectra of HXeC_4H . The absorptions at 1503.5, 1521.5, and 1532 cm^{-1} (1093, 1103.5, and 1111.5 cm^{-1} for DXeC_4D) decrease and the absorptions of 1545 and 1558.5 cm^{-1} (1120.5 and 1127.5 cm^{-1} for DXeC_4D) increase at higher temperature (see Figure 4 and Table 3). Simultaneously, HXeH (and DXeD) decomposes and its site structure changes as described elsewhere.^{37,40}

4. Discussion

The assignment of the observed absorptions to the novel rare-gas molecules HKrC_4H and HXeC_4H (see Table 3) is based on several facts. Because the obtained IR absorption spectra strongly depend on the matrix medium (Ar, Kr, and Xe), this suggests that the annealing-induced absorbers appearing specifically in Kr and Xe matrixes should contain Kr and Xe atoms. The rare-gas molecules have the typically strong H–Rg stretching absorptions, which makes them quite easily detectable,^{8,9} and the strongest bands observed in this study correspond well to the known characteristics of the H–Kr and H–Xe stretching modes. The observed extensive matrix-site splitting of the absorption bands is also very typical for the HRgY molecules.^{11,12,23} The rare-gas molecules usually decompose easily upon irradiation by light due to excitation to repulsive states.^{8,12,15,21,23,37} This behavior was found for both of the present absorbers: They decomposed efficiently after ~ 250 pulses (10 mJ/cm^2) at ~ 300 nm. In particular, using this selective photodissociation, we could reliably identify the weaker absorptions belonging to these absorbers (Table 3). The assignments are supported by the deuteration experiments.

The calculated spectra of HXeC_4H and HKrC_4H are in good agreement with the observed spectra. All computationally strong bands were found in the experiments, and these are, in addition to the H–Rg stretch, the H–C stretch and the C–C–H and C–C–C bendings. The harmonic MP2 H–Rg stretching frequencies are theoretically overestimated, but this is typical in the case of the HRgY molecules.^{9,41} This is most probably due to both an effect of the matrix surrounding and a lack of the theoretical accuracy.

The HRgC_4H molecules form presumably via the $\text{H} + \text{Rg} + \text{C}_4\text{H}$ reaction. Production of C_4H radicals occurs not only during photolysis but also in the annealing stage ($\text{H} + \text{C}_4$). It seems that the latter channel dominates because the amount of C_4 produced upon photolysis correlates with the amount of forming HRgC_4H and the C_4H concentration increases upon annealing. Furthermore, the annealing-induced formation of C_4H suggests that the HRgC_4 radicals do not form. To remind ourselves, the HXeCC radical was experimentally found,²¹ whereas HKrCC did not form,²³ and these results agreed with the theoretical data. We performed no calculations on the HRgC_4 radical because the results at the computational level used here could be unreliable as we found for HXeO and HXeCC earlier.^{13,21} It should be emphasized that the HRgC_4H molecules presumably form via a neutral channel as we have repeatedly discussed.^{9,14,42} It is an important question because the RgHRg^+ ions appear

usually during UV photolysis of HY in Rg matrixes, and the ionic channel for formation of HRgY is basically possible. In this study, when we photolyzed C_4H_2 in solid Kr at 240 and 250 nm, no production of KrHKr^+ was observed, whereas HKrC_4H efficiently formed upon annealing. Similarly, 193 nm photolysis of HCN in a Kr matrix did not produce KrHKr^+ ions, whereas the HKrCN molecules efficiently formed upon annealing.¹⁴ These observations confirm that the HRgY molecules form from neutral fragments instead of ionic channels involving the RgHRg^+ cations.

The detected change of the matrix-site structure of the absorption bands deserves discussion. We observed the decrease of some lower-frequency H–Rg stretching bands and the increase of other higher-frequency bands of HRgC_4H at higher-temperature annealing (above 40 and 55 K in Kr and Xe solids, respectively) as shown in Figures 3 and 4. The most detailed data were obtained for HXeC_4H (see Table 3). A similar thermal effect was also earlier observed for HArF ,¹¹ HKrF ,¹² and tentatively HXeD .³⁷ It was suggested that this effect is due to thermal relaxation of the species in a local energy minimum to a more stable configuration in the matrix surrounding. The same qualitative explanation is taken in the present case. It is reasonable that the long HRgC_4H molecules can easily be perturbed by the interaction with the matrix atoms. Importantly, for HXeC_4H , we observed the thermally induced modifications of all bands detected: the C–H stretching, C–C–C bending, and C–C–H bending modes in addition to the H–Xe stretching mode (see Table 3). It seems intuitively that the matrix-site splitting in the present case is caused mainly by surrounding-induced deformation of the whole molecule. For instance, its linearity may be perturbed. In any case, the HRgY molecules are very sensitive to the local matrix surrounding, especially to the complexation with an impurity.^{15–17}

The properties of the $\text{HRgC}_2\text{H}^{20–23}$ and HRgC_4H molecules are worth comparing. Most importantly, the HRgC_4H species appear to be more strongly bound than the analogues with two carbon atoms. This trend is indicated by the blue shift of the H–Rg stretching frequency for HRgC_4H which is computationally estimated to be $\sim +52$ and $+23$ cm^{-1} for the Kr and Xe species, respectively. In good agreement, experiments yield blue shifts between 34 and 75 cm^{-1} for HKrC_4H and from 17 to 73 cm^{-1} for HXeC_4H depending on the matrix-site band. The increasing stability of HRgC_4H is also shown by the shortening of the H–Rg bond (computationally by 0.02 and 0.01 Å for the Kr and Xe species, respectively). An important trend is the computational stabilization of the HRgC_4H as compared with the $\text{H} + \text{Rg} + \text{C}_4\text{H}$ asymptote: The stabilization energy increases by 0.59 and 1.06 eV for HKrC_4H and HXeC_4H as compared with the C_2 analogues. The charge distribution follows this stabilization trend: The computed (HRg) charges slightly increase for HRgC_4H (by 0.04 and 0.02 for the Kr and Xe species, respectively), and the negative charges of the carbon atoms have also increased by 0.04 for Kr and by 0.03 for Xe. In the case of HRgC_2H , the carbon atom vicinal to the Rg atom has 55% (Kr) and 61% (Xe) of the total negative charge of the two carbon atoms. The situation is similar in the case of HRgC_4H , where the carbon atom bound to the Rg atom has 41% and 51% of the total negative charge of the four carbon atoms for the Kr and Xe species, respectively. The two inner carbon atoms in HRgC_4H have 65% and 69% (for Rg = Kr

(40) Feldman, V. I.; Sukhov, F. F. *Chem. Phys. Lett.* **1996**, 255, 425.

(41) Lundell, J.; Chaban, G. M.; Gerber, R. B. *J. Phys. Chem. A* **2000**, 104, 7944.

(42) Pettersson, M.; Nieminen, J.; Khriachtchev, L.; Räsänen, M. *J. Chem. Phys.* **1997**, 107, 8423.

and Xe, respectively) of the total negative charge of the four C atoms. This indicates that in the case of the $C_{2n}H$ radical the electron affinity is localized at the “hydrogen-free” end. We expect that $HRgC_6H$ and $HRgC_8H$ are even more stable than $HRgC_2H$ and $HRgC_4H$ because the electron affinities of C_6H and C_8H are 3.8 and 3.9 eV, respectively, which are larger than those of C_2H and C_4H (~ 3 and 3.6 eV, respectively).²⁵ It seems that the $HRgC_{2n}H$ species are good candidates to form a stable bulk structure.

5. Conclusions

We reported here experimental and theoretical identification of the $HRgC_4H$ species ($Rg = Kr$ or Xe) formed from diacetylene and Rg atoms. The experimental synthesis includes UV photolysis of C_4H_2 in Rg matrixes and posterior annealing. The $HRgC_4H$ molecules are formed upon global diffusion of H atoms at ~ 30 and ~ 40 K in Kr and Xe solids, respectively, via the $H + Rg + C_4H$ reaction. The IR absorption bands of both $HKrC_4H$ and $HXeC_4H$ molecules exhibit extensive matrix-site structure, which undergoes modification upon higher-temperature annealing at above 40 and 55 K in Kr and Xe matrixes,

respectively. This interesting solid-phase process is presumably caused by extensive thermal relaxation of the local surrounding and shows the sensitivity of $HRgC_4H$ to the local matrix morphology.

The strongest IR absorption bands of $HRgC_4H$ molecules are the $H-Rg$ stretches with the most intense components at 1290 cm^{-1} for $HKrC_4H$ and 1532 cm^{-1} for $HXeC_4H$. These frequencies are higher than the corresponding values for $HRgC_2H$ found recently,^{21–23} suggesting enhanced stability of the larger molecules. This trend is supported by computational results, suggesting importantly that quite large organo-rare-gas molecules of this type could be very stable and the corresponding chemistry could be rich by analogy with fluorine-containing organoxenon compounds.

Acknowledgment. This work was supported by the Academy of Finland. H.T. thanks the Magnus Ehrnrooth foundation for financial support. The CSC-Center for Scientific Computing Ltd. (Espoo, Finland) is acknowledged for allocated computer time.

JA038610X